


Combinatorially Inducible RNA Interference Triggered by Chemically Modified Oligonucleotides

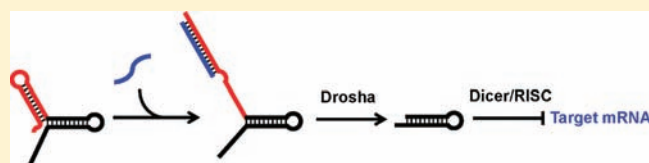
Deepak Kumar,[†] Sang Hoon Kim,^{†,‡} and Yohei Yokobayashi^{*,†}

[†]Department of Biomedical Engineering, University of California, Davis, 451 Health Sciences Drive, Davis, California, 95616, United States,

[‡]Department of Biology, Kyung Hee University, Seoul, 130-701, Republic of Korea

 Supporting Information

ABSTRACT: Chemically inducible RNA interference (RNAi) enables temporal and/or spatial control of virtually any gene, making it useful for study of gene functions, discovery of potential drug targets, and gene therapy applications. Here we describe a new inducible RNAi platform in which orthogonal chemically modified oligonucleotides are used to trigger silencing of two genes in a combinatorial manner. We developed a modular RNA architecture consisting of an oligonucleotide sensor stem-loop and an RNAi effector domain that is designed to undergo a structural shift upon addition of an oligonucleotide inducer. The induced structural change allows the RNA to be processed by the RNAi machinery, ultimately resulting in gene silencing of the target encoded by the RNAi effector module. Combinatorial regulation of multiple genes should accelerate studies of complex gene–gene interactions and screening of new drug targets.



INTRODUCTION

Since its initial discovery, RNAi has rapidly emerged as the dominating technique for downregulating specific gene expression in a variety of higher eukaryotes for basic studies and biomedical applications.^{1,2} However, constitutive gene knockdown precludes many applications of RNAi such as study of essential genes. Unregulated gene silencing is also undesirable for gene therapy applications. To meet these demands, a number of drug-inducible RNAi systems have been developed based on chemically inducible transcription factors and associated promoters that control the transcription of RNAi effectors such as short-hairpin RNAs (shRNAs).³ These platforms allow temporal and/or spatial regulation of a desired gene in cultured cells as well as in animals.

Applications of RNAi could expand significantly if multiple genes can be regulated independently and combinatorially by multiple, orthogonal inducers. For example, such a technology can be used to study how multiple genes interact to manifest a specific phenotype (e.g., diseases), or to screen for unknown combinations of potential drug targets that exhibit synthetic lethality.⁴ In principle, the existing drug-inducible RNAi platforms can be integrated to regulate multiple genes with multiple inducers. To the best of our knowledge, however, combinatorial silencing of more than one gene in an inducible manner has not been achieved. One can speculate on the considerable technical challenges to combine just two drug-inducible RNAi platforms, for example, the complexity and the large genetic size of the systems that include multiple transcription factors and promoters whose relative expression levels and activities may need to be finely optimized.

More recently, we and others have designed noncoding RNA transcripts whose RNAi activity can be posttranscriptionally

regulated by an exogenously added small molecule that directly interacts with the embedded RNA aptamer.^{5–9} We recently reported the only such system that activates (rather than inhibit) RNAi in response to a small molecule inducer by integrating an allosteric hammerhead ribozyme with a pri-miRNA analogue.⁸ In this strategy, a part of the RNAi-inducing pri-miRNA analogue is masked by a double-stranded stem which is conditionally exposed by an allosterically activated hammerhead ribozyme fused to the pri-miRNA analogue. Posttranscriptional nature of the induction mechanism offers new opportunities to design simpler and more efficient inducible RNAi platforms capable of combinatorial gene regulation.

In a slightly different approach, the Sando group described a conditional RNAi system that is activatable by a short synthetic RNA trigger.¹⁰ They designed derivatives of synthetic small interfering RNA (siRNA) duplexes that are commonly used to trigger RNAi whose hybridization (necessary for gene silencing) is controlled by an arbitrary RNA trigger. Although the Sando's system is not genetically encoded, the use of RNA (or other nucleic acids) as a trigger of RNAi may present an alternative strategy to chemically regulate RNAi in mammalian cells.

In this work, we developed a new platform called modified oligonucleotide-inducible RNAi (MONi–RNAi) that allows RNAi to be triggered by a small chemically modified oligonucleotide (MON). In contrast to Sando's system, our strategy uses genetically encoded RNA transcripts similar to our small molecule inducible RNAi strategies.^{5,8,9} Furthermore, we designed and constructed two orthogonal MONi–RNAi systems to combinatorially regulate two genes in cultured mammalian cells.

Received: November 30, 2010

Published: February 4, 2011

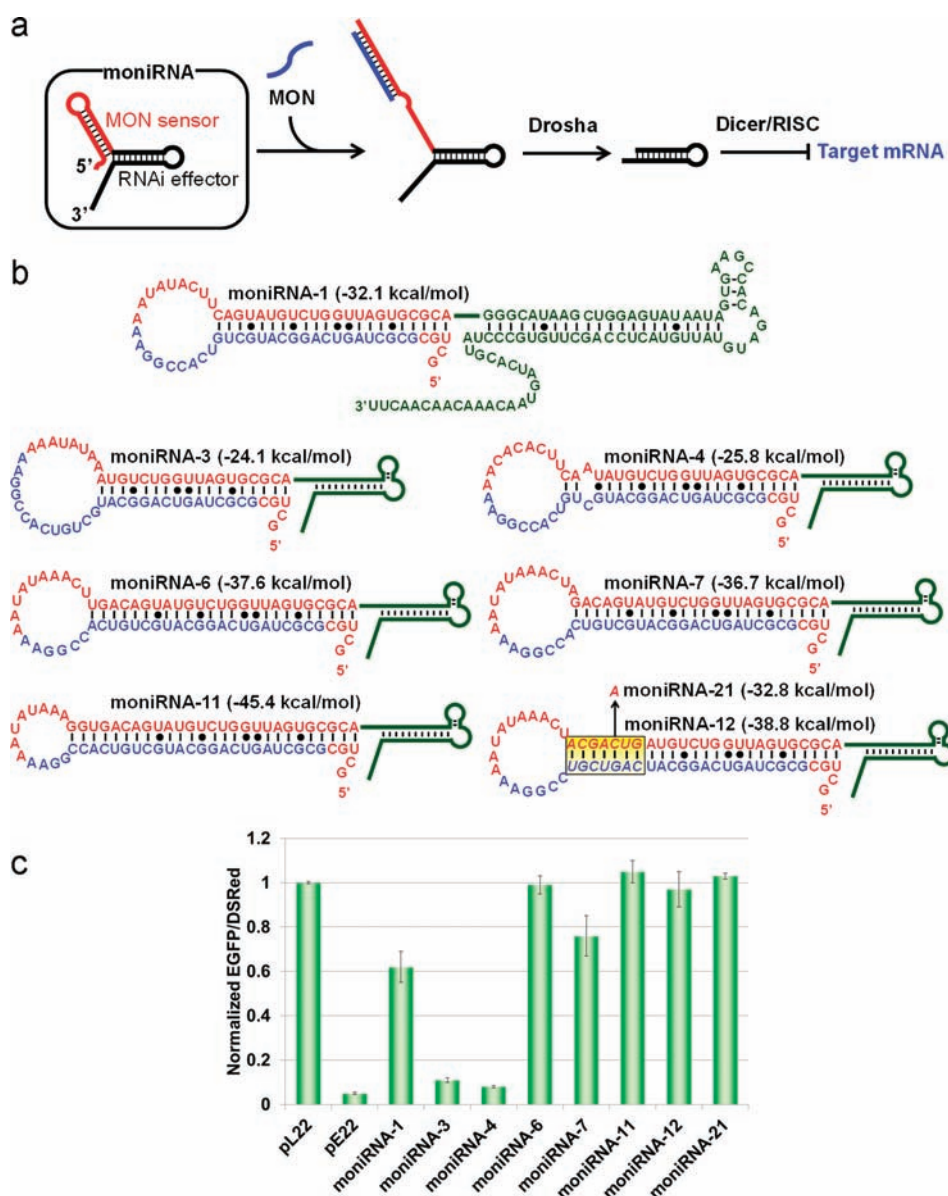


Figure 1. Design strategy of MONi-RNAi and optimization of the MON sensor domain. (a) Schematic illustration of MONi-RNAi strategy and mechanism. (b) Sequences and secondary structures predicted by Mfold¹¹ of moniRNAs with different MON sensor stem-loops. The calculated free energies (using Mfold) of the stem-loops are indicated in the parentheses. Blue bases indicate the complementary sequence that hybridizes with MON5 or MON6. (c) RNAi activities of moniRNAs depicted in b. pL22 (canonical pri-miRNA targeting firefly luciferase) and pE22 (canonical pri-miRNA targeting EGFP) represent negative and positive controls, respectively. The data shown in c are averages of triplicate transfections, and the error bars represent \pm SD.

RESULTS AND DISCUSSION

The overall strategy of MONi-RNAi is illustrated in Figure 1a. The noncoding RNA that is transcribed from the U6 promoter is named moniRNA (MON-inducible RNA) which contains two stem-loop domains. The 5' stem-loop functions as a MON sensor which hybridizes with the MON added as the inducer while the 3' stem-loop functions as the RNAi effector that is processed into siRNA. In the uninduced state, the stable MON sensor stem precludes the moniRNA from being processed by Droscha which recognizes long single-stranded regions flanking a short hairpin structure as its substrate.¹² In the presence of the MON inducer, however, the sensor stem opens to expose the 5' single-stranded region which allows Droscha to process the moniRNA into shRNA which eventually triggers RNAi (Figure 1a).

A key constraint of the moniRNA architecture is the MON sensor domain. The MON sensor stem-loop must be stable enough to resist processing by Droscha while unstable enough to be efficiently opened by the cognate MON inducer. Therefore, we first optimized the MON sensor stem-loop using an RNA effector domain that targets enhanced green fluorescent protein (EGFP). HEK293 cells were transfected with the plasmid mixture containing reporter plasmids that express EGFP and DsRed (pEGFP-N1 and pDsRed1-N1, respectively) and one of the moniRNA expression plasmids (pU6moniRNA-n) or controls (pE22: canonical pri-miRNA targeting EGFP, or pL22: canonical pri-miRNA targeting firefly luciferase, Figure S1, Supporting Information). Fluorescence levels of EGFP (targeted by moniRNA) and DsRed (used to normalize for transfection efficiency) were

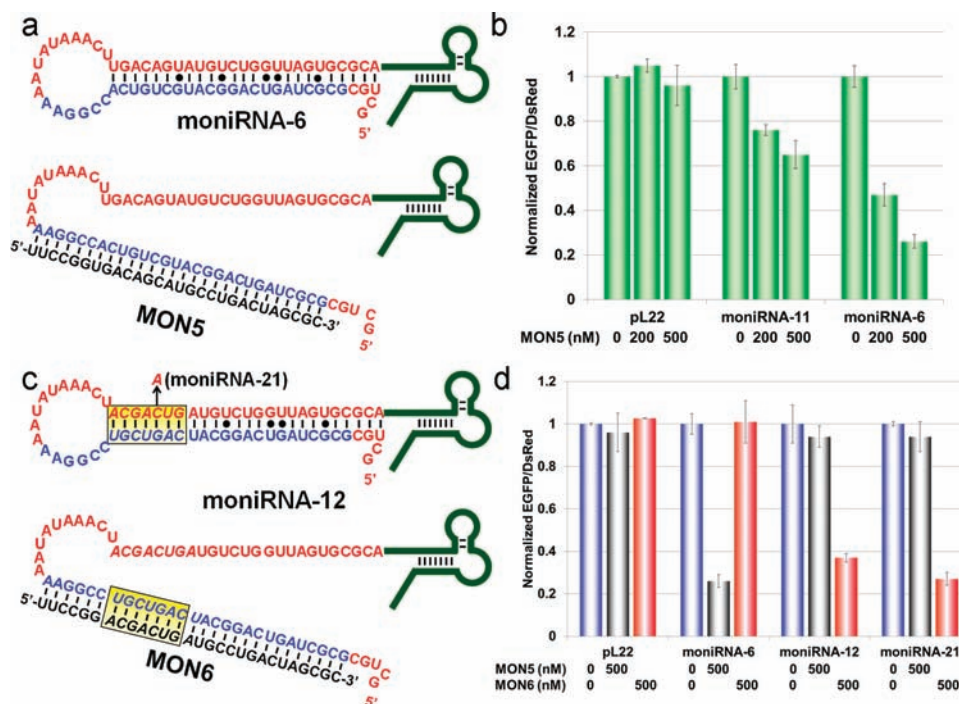


Figure 2. Induction of RNAi by MONs. (a) Uninduced and induced states of moniRNA-6 regulated by MON5. (b) Induction of RNAi from moniRNA-6 and moniRNA-11 by MON5. (c) Uninduced and induced states of moniRNA-12 and moniRNA-21 regulated by MON6. The yellow box indicates the sequence region that was shuffled from moniRNA-6/MON5 to enable orthogonal activation. (d) Specific induction of RNAi from moniRNAs triggered by MON5 (moniRNA-6) or MON6 (moniRNA-12, moniRNA-21). The data shown in b and d are averages of triplicate transfections, and the error bars represent \pm SD.

measured after 48 h. As expected, the less stable MON sensor stems (moniRNA-3, -4) resulted in uninduced RNAi that is indistinguishable from the positive control (pE22) (Figure 1b,c). However, progressive stabilization of the MON sensor stem revealed that the cells expressing moniRNA-6 and moniRNA-11 yielded EGFP levels comparable to the negative control (pL22), suggesting that these MON sensor stems are sufficiently stable to block RNAi (Figure 1b,c). In general, moniRNAs with higher MON sensor stem-loop stability showed weaker RNAi activity (Figure 1b,c). One exception was moniRNA-21 whose single base mutation from moniRNA-12 makes it less stable compared to moniRNA-7, yet no detectable RNAi was observed. From these results, it is possible that the efficiency of moniRNAs as Drosha substrates depend on more than the overall thermodynamic stability of the MON sensor stem-loops, perhaps involving the local stability or accessibility near the Drosha cleavage sites.

Next, we tested if these moniRNAs can be induced to knock-down EGFP expression by a MON inducer. We designed a 28-mer 2'-O-methyl (2'-OMe) oligonucleotide MON5 whose sequence is complementary to a part of the MON sensor stem domain as shown in Figure 2a. MON5 was transfected at different concentrations 4 h after the transfection of the plasmid mixture. As shown in Figure 2b, EGFP expression was diminished in the presence of MON5. Consistent with the expectations, MON5 induced stronger gene silencing from moniRNA-6, whose MON sensor stem is less stable compared to moniRNA-11 (Figure 2b). A shorter 22-mer oligonucleotide MON2 that lacks six bases at the 3' end of MON5 was able to induce RNAi from moniRNA-6 with moderately lower efficiency (Figure S2, Supporting Information). While there are numerous possibilities for further optimization of the MON size, chemistry, and delivery methods, we used 28-mer 2'-OMe

oligonucleotides as MON triggers to demonstrate MONi–RNAi functions in the remainder of this study.

We anticipated that the moniRNA architecture would retain high modularity of the MON sensor and the RNAi effector domains such that it would be straightforward to design orthogonal MON/MON sensor stem pairs that can be combined with arbitrary RNAi effector domains. To demonstrate this property, seven base pairs within the MON sensor stem of moniRNA-6 were shuffled to yield moniRNA-12 while preserving the overall RNA structure (Figure 2c). As a result of the sequence modification, MON5 failed to activate moniRNA-12 while MON6 that was designed to activate the altered MON sensor stem efficiently triggered RNAi (Figure 2d). The induction efficiency of moniRNA-12 by MON6 was moderately improved by fine-tuning the stability of the MON sensor stem (moniRNA-21), indicating further possibilities for optimization (Figure 2d). Overall, these results solidly suggest that orthogonal MON/MON sensor stem pairs can be designed with relative ease.

With two MON/MON sensor stem pairs in our hand, we designed a new moniRNA with the MON6-activated sensor stem-loop (from moniRNA-21) fused to an RNAi effector targeting DsRed (moniRNA-21–DsRed). Four plasmids (pEGFP-N1, pDsRed1-N1, pU6moniRNA-6, pU6moniRNA-21–DsRed) were cotransfected into HEK293 cells, and cellular fluorescence was observed under a fluorescence microscope in the absence and presence of the MON inducers (Figure 3a). The observed cellular fluorescence patterns further demonstrate that the MON inducers specifically activate RNAi from the cognate moniRNAs. Finally, the MON sensor stems were attached to RNAi effector domains targeting lamin A/C and vimentin to demonstrate the feasibility of the platform to regulate endogenous genes. Cells

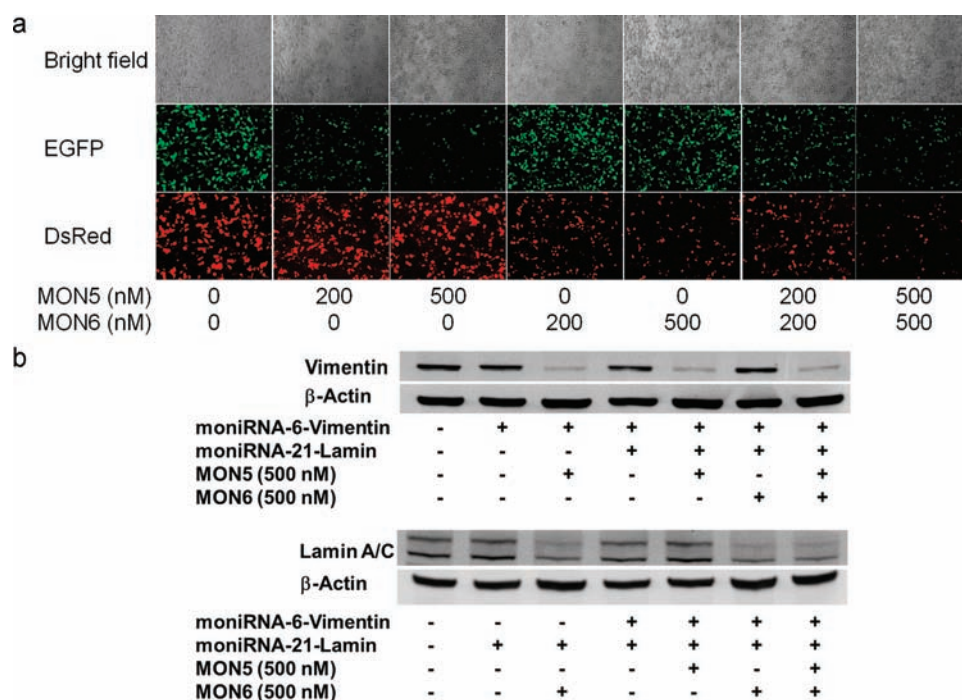


Figure 3. Combinatorial RNAi of exogenous and endogenous genes by two orthogonal MONi-RNAi systems. (a) HEK293 cells cotransfected with EGFP and DsRed expression plasmids and pU6moniRNA-6 and pU6moniRNA-21-DsRed were treated with MON5 and/or MON6 and examined by fluorescence microscopy. MON5 downregulated EGFP via pU6moniRNA-6 and MON6 downregulated DsRed via pU6moniRNA-21-DsRed. Expression levels of both EGFP and DsRed were suppressed when the cells were treated with both MON5 and MON6. (b) HEK293 cells cotransfected with pU6moniRNA-6-vimentin and pU6moniRNA-21-lamin were treated with MON5 and/or MON6 and the protein expression levels were analyzed by Western blot. MON5 triggered RNAi against vimentin, and MON6 triggered RNAi against lamin A/C. β -Actin was detected as loading and membrane transfer controls.

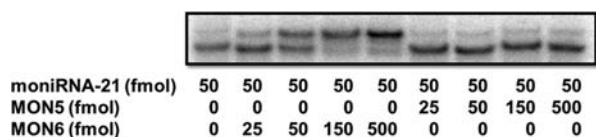


Figure 4. Hybridization of moniRNA and MON examined in vitro. Radiolabeled moniRNA-21 transcript prepared in vitro (100 fmol) was mixed with the indicated amounts of MON5 or MON6 in 10 μ L and incubated for 30 min at 37 $^{\circ}$ C. The samples (5 μ L per lane) were separated on a native 8% polyacrylamide gel and imaged. Significant electrophoretic mobility shift was observed for moniRNA-21 mixed with MON6, but not with MON5, confirming selective hybridization.

cotransfected with the two plasmids (pU6moniRNA-6-vimentin and pU6moniRNA-21-lamin) were treated with the MON inducer(s), and the protein levels were determined by Western blot analysis (Figure 3b). Again, expression levels of the two proteins were regulated combinatorially by the two orthogonal MON inducers in an expected fashion.

The ability of MONs to induce sequence specific hybridization and structural reorganization was confirmed in vitro by electrophoretic mobility shift assay (EMSA). In vitro transcribed moniRNA-21 (with EGFP-targeting RNAi effector domain) was radiolabeled and incubated with MON5 or MON6 at 37 $^{\circ}$ C for 30 min and separated in a native polyacrylamide gel. The mobility of moniRNA-21 completely shifted in the presence of 3-fold excess of MON6 while no significant shift was observed even in the presence of 10-fold MON5 (Figure 4).

Endogenous microRNAs (miRNA) are transcribed as longer primary transcripts that are posttranscriptionally processed by a

number of cellular factors such as Drosha and Dicer. Previously, we showed that processing of shRNA by Dicer can be chemically modulated by an RNA aptamer that is embedded in the loop region.^{5,9} However, this design strategy has only allowed inhibition of RNAi by the aptamer ligand. More recently, we designed a chemically inducible RNAi strategy that modulates the processing step catalyzed by Drosha by activating an aptamer-regulated allosteric ribozyme which releases the inhibitory RNA strand that masks the essential 5' single-stranded region of the Drosha substrate.⁸ MONi-RNAi adopts a similar yet distinct strategy to exploit the substrate recognition of Drosha by regulating the hybridization state of the 5' single-stranded region of Drosha substrate. These strategies based on the Drosha-mediated processing of RNAi effectors offer better isolation of the molecular sensing function from the RNAi function compared to the strategies involving the Dicer processing step.^{5,6,9} The modularity of the two functional domains of the moniRNA architecture was clearly demonstrated in the ability to target multiple genes by multiple MONs. Moreover, induction of structural reorganization driven by oligonucleotide hybridization is reminiscent of the DNA nanomachines that perform nanomechanical work using DNA hybridization as the driving force.^{13,14} In that sense, MONi-RNAi may be viewed as a genetically encoded RNA nanomachine with a biological function.

At first glance, the RNA-triggered RNAi system reported by the Sando group¹⁰ may appear similar to our MONi-RNAi. However, the two systems are highly distinct in their goals and functions. First, Sando's conditional RNAi system is not genetically encoded like moniRNA, but rather a mixture of two partially modified RNAs prepared in vitro. Second, their "trigger RNA"

was preannealed with the conditional RNAi construct prior to their transfection into the cells. Therefore, they have not yet demonstrated induction of RNAi by a trigger RNA (of synthetic or endogenous origin) in situ. Lastly, Sando's envisioned (but not yet achieved) goal is to activate RNAi by an endogenous mRNA while our aim is to use a set of orthogonal MONs to regulate multiple genes in a combinatorial manner.

The small genetic size and the posttranscriptional induction mechanism of MONi–RNAi provide additional advantages over the existing drug-inducible RNAi platforms based on engineered transcription factors and modified promoters.³ For example, moniRNAs may be transcribed from natural promoters such as tissue-specific or viral promoters to control when or where moniRNAs are expressed in vivo. Moreover, the lack of any exogenous protein components reduces the risk of immunological complications.

CONCLUSION

To our knowledge, MONi–RNAi described here is the first system to combinatorially silence more than one gene using multiple orthogonal inducers. The simple design principle of the MON inducer/MON sensor domain based on Watson–Crick base pairing should allow design of an even larger pool of orthogonally inducible systems. Combinatorial regulation of multiple genes in various combinations will enable researchers to probe complex genetic interactions that manifest various phenotypes, or to screen for potential drug targets that exhibit synthetic lethality.⁴ Alternatively, MONi–RNAi can serve as an input interface for synthetic gene circuits in mammalian cells such as the recently described RNAi-based logic circuits.¹⁵

Further optimization of the performance may be possible by improving the sequence and chemistry of moniRNA and MON inducer. In particular, MON inducer design can benefit from the extensive past and ongoing studies on chemistry, biology, and delivery technologies of chemically modified oligonucleotides driven by nucleic acid-based therapeutic strategies such as antisense and RNAi.^{16–19} With further improvements, we believe that MONi–RNAi will be a powerful tool that enables sophisticated manipulation of multiple genes for various applications.

EXPERIMENTAL SECTION

Plasmid Construction. Plasmids pEGFP-N1 and pDsRed1-N1 were obtained from Clontech. pSilencer 2.1-U6 hygro (Ambion) was used to construct pL22, pE22, and all moniRNA expression plasmids (pU6moniRNA-n) described in this work. The expression cassettes were cloned as previously described^{5,8} using synthetic oligonucleotides downstream of the U6 promoter. Targeting sequences for lamin A/C and vimentin were derived from previous reports.^{20,21} The predicted pri-miRNA analogue and moniRNA transcript sequences are summarized in Supporting Information.

Modified Oligonucleotides. MON2, MON5, and MON6 are 2'-OMe with the following sequences: MON2 5'-UUCCG GUGAC AGCAU GCCUG AC-3', MON5 5'-UUCCG GUGAC AGCAU GCCUG ACUAG GCG-3', MON6 5'-UUCCG GACGA CUGAU GCCUG ACUAG GCG-3'. The oligos were synthesized and purified by HPLC by Integrated DNA Technologies (IDT).

Cell Culture and Transfection. HEK293 cells were maintained in a 5% CO₂ humidified incubator at 37 °C in Dulbecco's modified Eagle's medium (DMEM) (Invitrogen) supplemented with 10% fetal bovine serum (FBS) (JR Scientific) and 1× antibiotic-antimycotic (Invitrogen). One day before transfection, HEK293 cells were trypsinized and diluted

1:7 with fresh medium, and 100 μL per well (2.5 × 10⁴ cells) were seeded onto 96-well plates. A plasmid mixture consisting of pEGFP-N1 (10 ng), pDsRed1-N1 (25 ng), and an appropriate pU6moniRNA-n plasmid (or pL22 or pE22 for controls, 100 ng) was cotransfected using 1 μL of PolyFect reagent (QIAGEN) per well. The medium was replaced with fresh medium 3 h after the initial transfection. After 1 h of incubation, an appropriate 2'-OMe oligonucleotide(s) was transfected at the indicated concentration using 2 μL of PolyFect reagent per well. The medium was replaced 4–5 h after the oligo transfection and further incubated for 48 h. Cellular fluorescence was measured as described below.

Fluorescence Measurements. Fluorescence measurements and data processing were performed as previously described.^{5,8} EGFP and DsRed fluorescence were measured on Safire2 microplate reader (Tecan) according to the manufacturer's instructions. Before measuring fluorescence intensity, the medium was removed from each well and washed with prewarmed phosphate-buffered saline (PBS) and incubated at 37 °C for 10 min in the instrument. Fluorescence intensity of EGFP was divided by that of DsRed to obtain EGFP/DsRed (DsRed fluorescence was used to account for variations in transfection efficiency), and the average values and standard deviations of EGFP/DsRed from triplicate samples were calculated. Next, the average values and the standard deviations were normalized against those from the cells transfected with pL22 (negative control).

Microscopic Examination. One day before transfection, 200 μL per well (5 × 10⁴ cells) of cells were transferred to 48-well plates. A plasmid mixture consisting of pEGFP-N1 (10 ng), pDsRed-N1 (25 ng), pU6moniRNA-6 (150 ng), and pU6moniRNA-21–DsRed (150 ng) was cotransfected using 2.5 μL of PolyFect reagent per well. The medium was replaced with fresh medium 3 h after the initial transfection. After 1 h of incubation, appropriate 2'-OMe oligonucleotide(s) was transfected at the indicated concentration using 5 μL of PolyFect reagent per well. The medium was replaced 4–5 h after the oligo transfection and further incubated for 48 h. Cellular fluorescence was examined by a fluorescence microscope, and the images were analyzed using SimplePCI Version 6 (Hamamatsu).

Western Blot Analysis. Antivimentin and antilamin A/C antibodies (mouse-derived, monoclonal) were purchased from BD Biosciences. Anti-β-actin (mouse-derived, monoclonal) was purchased from Sigma-Aldrich. The secondary antibody goat-derived horseradish peroxidase conjugate was purchased from Santa Cruz Biotechnology. Antivimentin, antilamin A/C, anti-β-actin, and antihorseradish peroxidase conjugate were diluted 1:8000, 1:250, 1:10,000, and 1:10,000, respectively, in TBS-T (20 mM Tris HCl pH 7.6, 150 mM NaCl, 0.1% Tween 20) buffer.

One day before transfection, 2 mL per well (6 × 10⁵ cells) of cells were transferred to six-well plates. Plasmids pU6moniRNA-6–vimentin (1.5 μg) and/or pU6moniRNA-21–lamin (1.5 μg) were transfected using 20 μL of PolyFect per well. The medium was replaced with fresh medium 3 h after the initial transfection. After 1 h of incubation, the cells were transfected with an appropriate concentration of 2'-OMe oligonucleotide(s) using 30 μL of PolyFect reagent per well. The medium was replaced 4–5 h after the oligo transfection and further incubated for 48–60 h. The cells were harvested and lysed in lysis buffer (150 mM NaCl, 5 mM EDTA [pH 8], 1% Triton X-100, 0.1% SDS, 50 mM Tris [pH 8], 5 mM DTT, and 1× protease inhibitor [Roche Applied Science]) for 10 min on ice, and proteins were recovered after centrifugation of the lysate. The total protein concentration was measured using a NanoDrop 2000 (Thermo Scientific) spectrophotometer by the Bradford method. Total proteins were separated at 35 mA for 30 min on 12% MINI PROTEAN precast gel (Bio-Rad) using 1× Tris-Glycine-SDS buffer pH 8.3 (25 mM Tris, 192 mM glycine, and 0.1% SDS) for the detection of vimentin (10 μg total proteins) and lamin A/C (50 μg total proteins). The samples were transferred onto a nitrocellulose membrane

(Thermo Scientific) using 1× Tris-Glycine blotting buffer pH 8.3 (25 mM Tris, 192 mM glycine, 20% methanol). The membrane was blocked with 5% milk in TBS-T buffer and incubated with a primary antibody (antivimentin: 1 h, antilamin A/C: overnight, anti-β-actin: 30 min). After washing (2 × 15 min), the membrane was incubated with the secondary antibody (1:10 000) for 45 min. The membrane was washed again and imaged using ECL Plus reagent (GE Healthcare) on a Storm 860 Molecular Imager (Molecular Dynamics).

Electrophoretic Mobility Shift Assay (EMSA). RNA corresponding to the transcript expressed from pU6moniRNA-21 (with EGFP-targeting shRNA sequence) was synthesized by in vitro transcription using a template generated from PCR according to the instruction of MEGAshortscript kit (Ambion). The predicted transcript sequence is 5′-GGGCUGCGCG CUAGUCAGGC AUCAGUCGUC CGGAAA-AUAU AAACUACGAA UGAUGUCUGG UUAGUCGCGCA GGCC-AUAAGC UGGAGUAUA UAGUGAAGCC ACAGAUGUAU UG-UACUCCAG CUUGUGCCCU AUGCACUAGU AACAAACAAC AAC-3′. The RNA was purified by PAGE and dephosphorylated using Antarctic Phosphatase (New England Biolabs). The dephosphorylated RNA was labeled at the 5′ position with [γ - 32 P] ATP (Perkin-Elmer) using T4 polynucleotide kinase (New England Biolabs). The labeled RNA (100 fmol) was incubated with MON5 or MON6 at various concentrations at 37 °C for 30 min in 10 μ L of hybridization buffer (5 mM Tris HCl pH 8, 3 mM MgCl₂, 10 mM NaCl, and 100 mM KCl). The mixture (5 μ L) was separated on a native 8% polyacrylamide gel using 0.5× THE buffer (17 mM Tris, 33 mM HEPES, 0.05 mM EDTA). The gel was dried and exposed on a Storage Phosphor Screen (GE Healthcare) and imaged using a Storm 860 Molecular Imager.

■ ASSOCIATED CONTENT

S Supporting Information. Figures and a list of RNA sequences described in this article. This material is available free of charge via the Internet at <http://pubs.acs.org>.

■ AUTHOR INFORMATION

Corresponding Author

yoko@ucdavis.edu

■ ACKNOWLEDGMENT

This work was supported by National Science Foundation (CBET-0755053). S.H.K. was supported by Nuclear R&D Program through the National Research Foundation of Korea funded by the Ministry of Education, Science, and Technology (2010-0017585 and 2010-0017418).

■ REFERENCES

- (1) Hannon, G. J.; Rossi, J. J. *Nature* **2004**, *431*, 371–378.
- (2) Meister, G.; Tuschl, T. *Nature* **2004**, *431*, 343–349.
- (3) Wiznerowicz, M.; Szulc, J.; Trono, D. *Nat. Methods* **2006**, *3*, 682–688.
- (4) Kaelin, W. G., Jr. *Nat. Rev. Cancer* **2005**, *5*, 689–698.
- (5) An, C. I.; Trinh, V. B.; Yokobayashi, Y. *RNA* **2006**, *12*, 710–716.
- (6) Beisel, C. L.; Bayer, T. S.; Hoff, K. G.; Smolke, C. D. *Mol. Syst. Biol.* **2008**, *4*, 224.
- (7) Beisel, C. L.; Chen, Y. Y.; Culler, S. J.; Hoff, K. G.; Smolke, C. D. *Nucleic Acids Res.* **2010** (doi: 10.1093/nar/gkq954).
- (8) Kumar, D.; An, C. I.; Yokobayashi, Y. *J. Am. Chem. Soc.* **2009**, *131*, 13906–13907.
- (9) Tuleuova, N.; An, C. I.; Ramanculov, E.; Revzin, A.; Yokobayashi, Y. *Biochem. Biophys. Res. Commun.* **2008**, *376*, 169–173.
- (10) Masu, H.; Narita, A.; Tokunaga, T.; Ohashi, M.; Aoyama, Y.; Sando, S. *Angew. Chem., Int. Ed.* **2009**, *48*, 9481–9483.

- (11) Zuker, M. *Nucleic Acids Res.* **2003**, *31*, 3406–3415.
- (12) Zeng, Y.; Cullen, B. R. *J. Biol. Chem.* **2005**, *280*, 27595–27603.
- (13) Dittmer, W. U.; Reuter, A.; Simmel, F. C. *Angew. Chem., Int. Ed.* **2004**, *43*, 3550–3553.
- (14) Yurke, B.; Turberfield, A. J.; Mills, A. P., Jr.; Simmel, F. C.; Neumann, J. L. *Nature* **2000**, *406*, 605–608.
- (15) Rinaudo, K.; Bleris, L.; Maddamsetti, R.; Subramanian, S.; Weiss, R.; Benenson, Y. *Nat. Biotechnol.* **2007**, *25*, 795–801.
- (16) Behlke, M. A. *Oligonucleotides* **2008**, *18*, 305–319.
- (17) Kurreck, J. *Eur. J. Biochem.* **2003**, *270*, 1628–1644.
- (18) Marlin, F.; Simon, P.; Saison-Behmoaras, T.; Giovannangeli, C. *Chembiochem* **2010**, *11*, 1493–1500.
- (19) Prakash, T. P.; Bhat, B. *Curr. Top. Med. Chem.* **2007**, *7*, 641–649.
- (20) Elbashir, S. M.; Harborth, J.; Lendeckel, W.; Yalcin, A.; Weber, K.; Tuschl, T. *Nature* **2001**, *411*, 494–498.
- (21) Harborth, J.; Elbashir, S. M.; Beichert, K.; Tuschl, T.; Weber, K. *J. Cell Sci.* **2001**, *114*, 4557–4565.